Supercond. Sci. Technol. 12 (1999) 809–812. Printed in the UK PII: S0953-2048(99)05016-2

High-T_c SQUID microscope with sample chamber

Saburo Tanaka, Osamu Yamazaki, Ryoji Shimizu and Yusuke Saito

Ecological Engineering, Toyohashi University of Technology, Hibarigaoka Tempaku-cho Toyohashi Aichi 441-8580, Japan

Received 22 June 1999

Abstract. We have designed and constructed a high-T_c superconducting quantum interference device (SQUID) microscope with a sample chamber isolated by a shutter. It can image magnetic distributions of samples at both room temperature and 77 K. According to our scheme, the separation of the sample from the SQUID can be less than a few micrometres, in principle. We have successfully imaged a trapped flux in a $YBa_2Cu_3O_{7-y}$ thin-film ring at 77 K and a printout of a laser printer at room temperature.

1. Introduction

It is important to image weak magnetic fields by a superconducting quantum interference device (SQUID) microscope not only for non-destructive evaluation (NDE) but also for studies in physics such as vortex dynamics [1–6]. Although a high-T_c SQUID is typically one order of magnitude less sensitive than a 4.2 K low-T_c SQUID, there are many advantages of using high-T_c SQUIDs such as easy thermal insulation, easy handling and low running cost [7, 8]. High-T_c SQUID microscopes reported to date are classified into two types; one is for cold samples (77 K) and the other is for room-temperature samples. Black and coworkers pioneered the use of high-T_c SQUIDs operated at liquid N_2 temperature to evaluate cold samples [9, 10]. Recently, a high-T_c SQUID microscope for room-temperature samples has been developed and used for biological applications [11, 12]. In the SQUID microscope for cold samples, the accumulation of ice on the sample is one of the major problems because the SQUID and the sample are immersed in liquid nitrogen. An obvious disadvantage of the system is that the time required for thermal cycling is long. In the SQUID for room-temperature samples, there is no icing problem, but the separation of the sample from the SQUID cannot be less than several tens of micrometres, because of the presence of a window isolating the sample from the cold SQUID in vacuum. We have developed a high-T_c SQUID microscope with a sample chamber isolated by a shutter gate. After pumping both the cryostat and the sample chamber, the shutter is opened and the sample is positioned as close as possible to the SQUID. Thus the microscope becomes 'windowless'.

According to our scheme, the temperature of the sample can be changed and the distance between the sample and the SQUID can be reduced to several micrometres, in principle [13]. After finishing the evaluation, the shutter will be closed again. We present here the design of our windowless high-T_c SQUID microscope and some results of 2D field images.

2. Construction of microscope

We used a $YBa_2Cu_3O_{7-y}$ (YBCO) SQUID magnetometer for the system. This SQUID is a product of Sumitomo, Electric Ind, Ltd [14]. The junctions utilized in the SQUID are of the step-edge type. The washer size of the SQUID is about 2.5 mm × 2.5 mm and the effective area is 0.11 mm^2. The inner hole is rectangular and its size is 5 μm × 200 μm.

The configuration of the microscope is shown in figures 1 and 2. Most parts of the cryostat are made of G-10 fibreglass and Delrin. They are nonmetallic except for a copper reservoir, liquid N_2 filling tubes and stainless steel bellows. The size of the cryostat is 250 mm in diameter and 280 mm in height.

The cryostat contains a liquid N_2 copper reservoir, the volume of which is 0.8 l. The reservoir is superinsulated by 30 layers of single-sided aluminium evaporated Mylar sheet. The inside of the cryostat can be evacuated by a vacuum pump and sealed off by an o-ring valve. The SQUID chip is silver pasted on top of a sapphire rod thermally anchored with the liquid N_2 reservoir. This cryostat can keep liquid N_2 for 17.5 hours. The SQUID is 50 mm away from the metallic reservoir. A modulation coil and a heater are installed in the upper end of the sapphire rod. A copper wire step-up transformer is glued tightly to the top of the copper reservoir. Electrical contacts to the SQUID chip are made by applying conductive silver paint to the bonding pads and the side of the SQUID chip.

The size of a sample chamber is 100 mm diameter ×60 mm height. The details of the chamber are shown in figure 2. The chamber consists of top and bottom fibreglass discs with a hole at the centre and a quartz cylindrical glass. These discs are sealed by o-rings. The bottom plate is coupled to the top plate of the cryostat through a fibreglass tube. The chamber with the cryostat looks like a 'double-decker'. The position of the sample chamber can be changed by turning three positioning screws set at the bottom of the sample chamber. A sample holder made of copper, which contains

0953-2048/99/110809+04$30.00

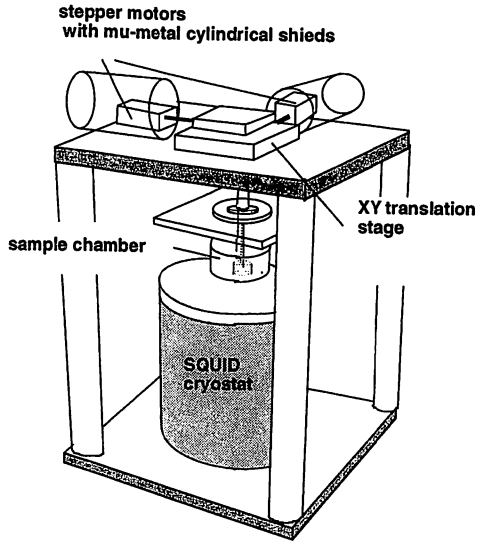

Figure 1. Side view of microscope. The sample chamber is connected to the cryostat, which includes a high-T_c SQUID chip. The sample holder is suspended from the XY translation stage. The stage can be driven by stepper motors. The frame consists of 50 mm diameter × 500 mm height Derlin columns and 20 mm thick 420 × 420 mm^2 aluminium alloy plates.

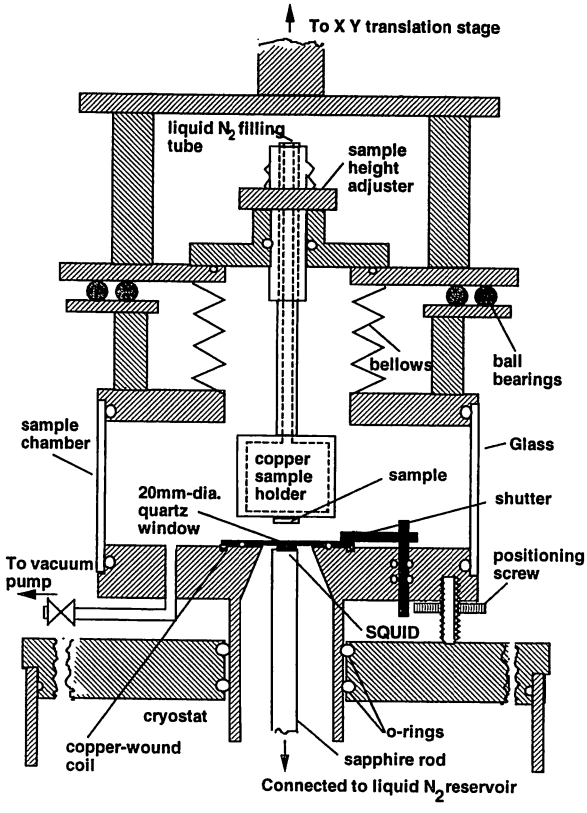

Figure 2. Detailed side view of sample chamber. The sample chamber and the cryostat can be separately evacuated. The shutter gate is installed between them. Motion can be controlled from the outside. The copper sample holder can be cooled by filling it with liquid nitrogen.

10 ml of liquid N_2, is centred on top of the chamber via stainless steel bellows. The vertical position of the holder can be adjusted by a height adjuster. The upper end of the bellows is connected to an aluminum alloy disc, which is placed on a flat plate via steel ball bearings. Thus, the disc with the sample

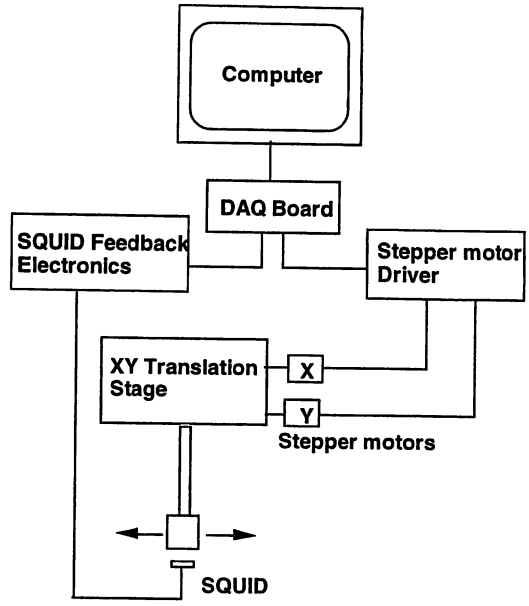

Figure 3. Schematic layout of electronics and data acquisition system. The signal voltage is coupled to an A/D interface board (NI-1200) and stored in a Macintosh 7200/90 computer. The program controlling the system is homemade and based on LabVIEW 4.0 (National Instruments).

holder can be moved smoothly in the X and Y directions with low friction. A 20 mm diameter quartz vacuum window shutter, which can be opened and closed from outside the sample chamber, is installed on the bottom disc. When it is closed, one can independently evacuate the sample chamber from a vacuum pump-out flange. A 20 mm diameter copper-wound coil, which can generate a known magnetic field to the sample, is equipped around the window hole.

The sample holder is connected to an XY translation stage placed on an upper 20 mm thick aluminum alloy table supported by four 60 mm diameter Delrin columns. The stage is made of aluminum alloy and driven by stepper motors, and is surrounded by a 1 mm thick mu-metal cylindrical shield to suppressed noise generated by the stepper motors. The minimum step size is 1.4 μm. the wobbling of the X direction screw is somewhat large and about 100 μm, though that of the Y direction is less than 10 μm. The maximum scan range is 10 × 10 mm^2 and the maximum scan speed is 1.2 mm s^{-1}.

The SQUID is operated in a flux-locked loop with a flux modulation frequency of 100 kHz. R_f/M_f is 1.7 V ϕ_0^{-1}, where R_f is the feedback resistance of the system and M_f is the mutual inductance between the SQUID and the modulation coil. The magnetic flux noise $S\phi^{1/2}(f)$ is 80 $\mu\phi_0$ Hz$^{-1/2}$ at 1 Hz and 40 $\mu\phi_0$ Hz$^{-1/2}$ in the white noise region. The schematic layout of the electronics and the data acquisition system is shown in figure 3. The output voltage V_{out} of the SQUID electronics is low-pass filtered at a frequency of 10 Hz. The signal voltage is coupled to an A/D interface board (NI-1200) and stored in a Macintosh 7200/90 computer. The computer also supplies pulses to the stepper motors that drive the translation stage. The program controlling the system is homemade and based on LabVIEW 4.0 (National Instruments). The signal data are converted into false colour contour images by the imaging software 'Spyglass'.

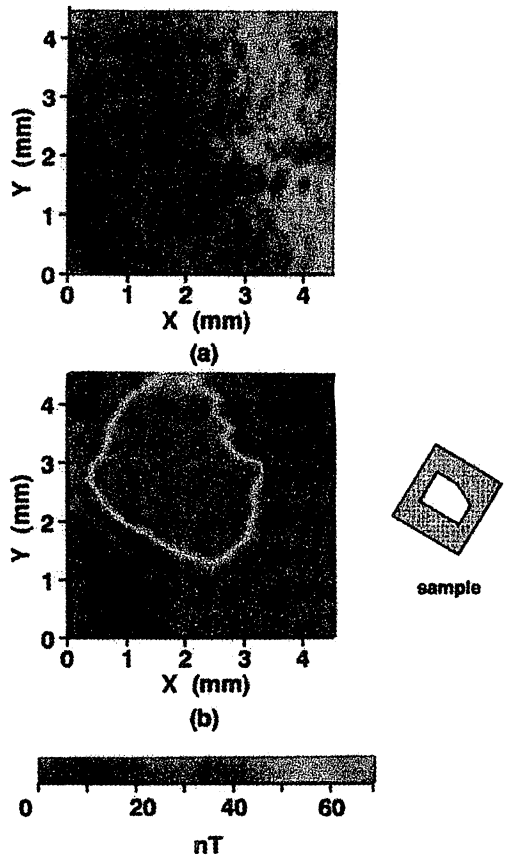

Figure 4. (a) 2D magnetic field image of YBCO thin-film ring at room temperature. Field distribution is caused by remanent field from metallic components comprising the microscope. (b) Field image of YBCO ring at 77 K. The magnetic field generated by the trapped flux is about 60 nT, which corresponds to 14 ϕ_0.

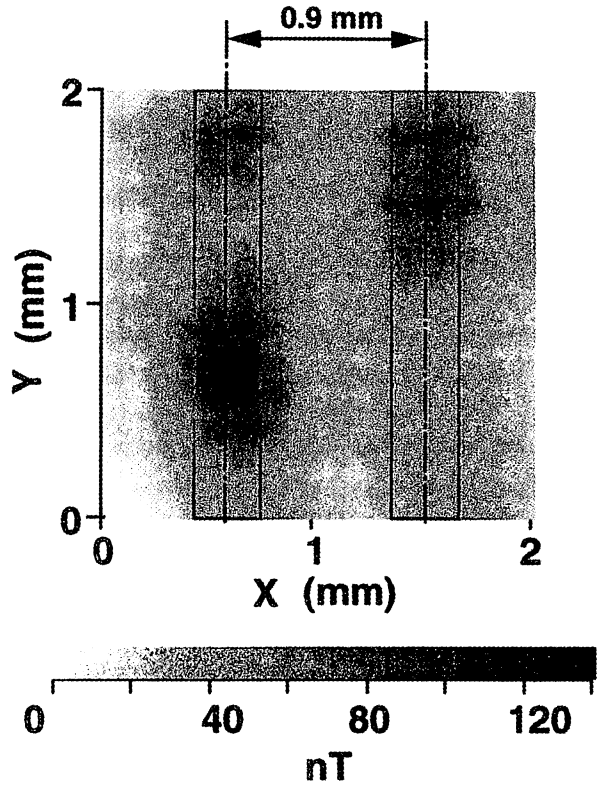

Figure 5. Image of a printout line pattern of a laser printer *Canon Laser Shot* and it's original pattern. The ink contains magnetic particles. The line separation is 0.9 mm. The dotted line shows the solid pattern area and the width is 0.3 mm.

3. Experimental and discussion

We performed all of the measurements in a magnetically shielded room with a shielding factor of −50 dB for 0.1 Hz. A YBCO superconducting thin-film ring with outer dimensions of about 1.3 × 1.4 mm^2 and inner dimensions of about 0.7 × 0.8 mm^2 was prepared for imaging. It was put on the copper holder by applying a silver paste, which made good thermal contact. After pumping out the cryostat, SQUID was cooled down by filling liquid N_2 to the reservoir. Then the sample chamber was separately evacuated so that the pressure of the chamber became the same as that of the SQUID cryostat. Opening the shutter, the positioning screws were mated so that the SQUID and the sample became parallel and as close as possible to each other. The separation of the sample from the SQUID was about 100 μm. Firstly, the sample was scanned at room temperature in the range of 4.5 × 4.5 mm^2. The scan rates along the X and Y axes were 1.11 mm s^{-1} and 0.225 mm step, respectively. The sampling rate was 10 s^{-1} in the X axis scan. This implies that the number of data is 40 × 20 points. Figure 4(a) shows a 2D magnetic field image of the sample at room temperature. A field inhomogeneity from lower left corner to upper right corner exists. This inhomogeneity may be caused by the remanent field from the metallic components comprising the microscope, such as steel ball bearings or stainless steel bellows. The field variation from the minimum to the maximum in the region is about 60 nT. The YBCO thin-film ring was cooled to 77 K and then scanned over. No magnetic field was applied to the sample while cooling. The produced 2D image is shown in figure 4(b). The shape of the sample is shown on the right in the same scale. The trapped flux inside the ring could be clearly seen, though no field was applied while cooling. The magnetic field generated by the trapped flux is about 60 nT, which corresponds to 14 ϕ_0, where ϕ_0 is a flux quantum. This trapped image is caused by the inhomogeneity of the environmental field. The jagged line along the Y axis is due to the backlash from the X direction. The reasons why the image is rounded and its size is larger than the real sample are explained by the size of the SQUID (2.5 mm × 2.5 mm) and the separation of the sample from the SQUID. Since the space resolution is restricted by the sensing area of the SQUID, it should be small to obtain good space resolution.

We could not reduce the distance between the SQUID and the sample to less than 100 μm because of the difficulty in closing them in parallel, though the distance can be less than a few micrometres in principle. Therefore, the field image in the hole is broadened and the area looks larger than that of the real sample. To solve this problem, the adjusting mechanism should be improved. After the measurement, the sample holder was warmed up to room temperature by inserting a wire heater into the sample holder. It took only 5–6 minutes to warm it up. Problems such as icing were not observed.

We tried to scan a stripe-shaped printout of a laser printer, of which the ink contained magnetic particles. In order to obtain good resolution, the printout sample was almost

touched to the SQUID. The scan range was 2 mm × 2 mm. The resulting image is shown in figure 5. The separation of the original pattern is 0.9 mm and width of the solid area is 0.3 mm. In this case, the broadness of the pattern was improved. This means that the separation between the sample and the SQUID is an important factor to obtain a good space resolution.

4. Conclusion

A high T_c SQUID microscope with a sample chamber isolated by a shutter was constructed. According to our scheme, the separation of the sample from the SQUID can be several micrometres, in principle. The other advantage of the system is that the required time for thermal cycling can be reduced without icing. Samples were measured at both room temperature and 77 K. A trapped flux in a YBCO thin-film ring could be imaged. By bringing into partial contact the sample on the SQUID, the space resolution was improved. When we imaged a magnetic printout line pattern with separation of 0.9 mm, the broadness of the pattern was dramatically improved.

Acknowledgments

We thank Mr M Kanamori for writing the LabVIEW program. This work was partially supported by a Grant-in-Aid for Scientific Research on Priority Area (A) from the Ministry of Education, Science, Sports and Culture of Japan.

References

[1] Donaldson G, Evanson S, Otaka M, Hasegawa K, Shimizu T and Takaku K 1990 Use of SQUID magnetic sensor to detect aging effects in duplex stainless steel *Br. J. NDT* **32** 238

[2] Weinstock H 1993 Prospects on the application of HTS SQUID magnetometry to nondestructive evaluation (NDE) *Physica* C **209** 269

[3] Tsuei C C, Kirtley J R, Chi C C, Lock See Yu-Jahnes, Gupta A, Shaw T, Sun J Z and Ketchen M B 1994 Pairing symmetry and flux quantization in, a tri-crystal superconducting ring of $YBa_2Cu_3O_7$ *Phys. Rev. Lett.* **73** 593

[4] Vu L N, Wistrom M S and Van Harlingen D J 1993 Imaging of magnetic vortices in superconducting networks and clusters by scanning SQUID microscopy *Appl. Phys. Lett.* **63** 1693

[5] Kasai N, Ishikawa N, Yamakawa H, Chinone K, Nakayama S and Odawara A 1997 Nondestructive detection of dislocations in steel using a SQUID gradiometer *IEEE Trans. Appl. Supercond.* **7** 2315

[6] Morooka T, Nakayama S, Odawara A, Ikeda M, Tanaka S and Chinone K 1999 Micro-imaging system using scanning DC-SQUID microscope *IEEE Trans. Appl. Supercond.* **9** at press

[7] Tanaka S, Itozaki H, Toyoda H, Harada N, Adachi A, Okajima K and Kado H 1994 Four-channel $YBa_2Cu_3O_{7-y}$ dc SQUID magnetometer for biomagnetic measurement *Appl. Phys. Lett.* **64** 514

[8] Wikswo J P 1995 SQUID magnetometers for biomagnetism and nondestructive testing: important questions and initial answers *IEEE Trans. Appl. Supercond.* **5** 74

[9] Black R C, Mathai A, Wellstood F C, Dantsker E, Miklich A H, Nemeth A H, Kingston J J and Clarke J 1993 Magnetic microscopy using a liquid nitrogen cooled YBCO SQUID *Appl. Phys. Lett.* **62** 2128

[10] Black R C, Wellstood F C, Dantsker E, Miklich A H, Kingston J J, Nemeth D T and Clarke J 1994 Eddy-current microscopy using a 77 K superconducting sensor *Appl. Phys. Lett.* **64** 100

[11] Lee T S, Dantsker G and Clarke J 1996 High-transition temperature SQUID microscope *Rev. Sci. Instrum.* **67** 4208

[12] Shaw T, Schlenga K, McDermott R, Clarke J, Chen J W, Kang S-H and Morris J W Jr 1999 High-T_c SQUID microscope study of the effects of microstructure and deformation on the remanent magnetization of steel *IEEE Trans. Appl. Supercond.* **9** at press

[13] Tanaka S, Yamazaki O, Shimizu R and Saito Y 1999 Windowless high T_c superconducting quantum interference device microscope *Japan. J. Appl. Phys.* **38** L505

[14] Catalogue on web page: `http://squid.sei.co.jp`. E-mail address: `squid@info.sei.co.jp`